Journal of Chemical Health Risks

www.jchr.org

JCHR (2025) 15(6), 3715-3722 | ISSN:2251-6727

Development of Activated carbon based $CeNiO_3$ Nanocomposite via Green Synthesis for the Applications of Photocatalytic Degradation

Kovendhan S [1] and Sheela R [2*]

[1]Research Scholar, Department of Civil Engineering Annamalai University, Annamalai Nagar, Chidambaram Tamilnadu, India

[2*]Associate Professor, Department of Civil Engineering Annamalai University, Annamalai Nagar, Chidambaram Tamilnadu, India

(Received: 05 November 2025 Revised: 15 November 2025 Accepted: 23 November 2025)

KEYWORDS

$CeNiO_3$ nanomaterials; Green synthesis; Photocatalysis; Adsorption; Wastewater treatment.

ABSTRACT:

Green-synthesized $CeNiO_3$ nanoparticles were effectively produced using Evodia and Azadirachta indica leaf extracts as environmentally benign reducing and stabilizing agents for photocatalytic and adsorption applications. The synthesis consisted on complexing cerium and nickel nitrate precursors with plant phytochemicals, followed by regulated heat treatment to get phase-pure perovskite $CeNiO_3$. X-ray diffraction investigation verified the establishment of a crystalline $CeNiO_3$ structure devoid of secondary contaminants. FTIR spectra indicated distinct Ce–O and Ni–O vibrations, as well as surface hydroxyl groups. SEM pictures showed nanoscale particles that were stuck together and had rough surfaces. EDS analysis confirmed the consistent elemental distribution of Ce, Ni, and O. UV–visible diffuse reflectance spectroscopy showed that the material absorbed a lot of visible light and had a smaller band gap. This was because the green synthesis technique created oxygen vacancies and mixed valence states. The synthesized $CeNiO_3$ exhibited a pronounced capacity to adsorb organic dye pollutants in the absence of light, thereafter undergoing efficient photocatalytic destruction upon exposure to visible light. This approach of combining adsorption and photocatalysis made it easier to remove pollutants and made it easy to use again. So, research suggests that $CeNiO_3$ nanoparticles generated in an ecologically acceptable way might be used for long-term wastewater treatment.

Introduction:

When NiO and $CeNiO_3$ nanoparticles are subjected to light energy larger than or equal to their band gap energy, conduction band electrons (e-) and valence band holes (h+) are produced, in accordance with the actual process of methylene blue dye degradation. The production of hydroxyl radicals mediates the oxidation of organic molecules, while the production of superoxide radicals promotes the reduction and oxidation processes[1]. The idea that hydroxyl radicals are the source of the oxidation pathway of chemical substances that is started by heterogeneous photocatalysis. The photogenerated electrons may mix with electron acceptors like $O2.^-$ adsorbed on the surface or dissolved in water, or the dye may be reduced to the superoxide radical anion $O2.^-$ [2]. The photogenerated holes may oxidize organic molecules by reacting with OH- or H_2O to generate.OH radicals. The OH- radical may transform most MB into non-toxic byproducts such CO_2, H_2O, and mineralized product because of its potent oxidizing capabilities [3,4].

Materials and Methods

Materials

Cerium nitrate hexahydrate [$Ce(NO_3)_3 \cdot 6H_2O$] and nickel nitrate hexahydrate [$Ni(NO_3)_2 \cdot 6H_2O$] were used as the starting materials. Plant leaves, such as those from Evodia or Azadirachta indica, were harvested and subsequently employed in the synthesis of the plant extract. All reagents were of analytical grade and were utilized without any additional purification steps.

Journal of Chemical Health Risks

www.jchr.org

JCHR (2025) 15(6), 3715-3722 | ISSN:2251-6727

Deionized water was the sole solvent employed in all experimental procedures.

Preparation of Plant Extract

Fresh plant leaves underwent a thorough washing with distilled water to eliminate contaminants before being shade-dried. Subsequently, the dried leaves were finely chopped and subjected to boiling in deionized water at a temperature range of 60–80 °C for a duration of 30–45 minutes. The resulting extract was then filtered using Whatman No.1 filter paper and subsequently stored at 4 °C for subsequent applications.

Green Synthesis of NiO Nanoparticles

A 0.1 M aqueous solution of nickel nitrate hexahydrate was prepared and heated while stirring. The plant extract was then added dropwise to the nickel nitrate solution, causing a color change that indicated nanoparticle formation. The reaction mixture was kept at a temperature between 70 and 80 °C for 2 to 3 hours. The resulting precipitate was centrifuged and then washed several times with distilled water and ethanol to remove impurities. The washed product was dried at 80 °C and then calcined at 400–500 °C for 3 to 4 hours to create crystalline NiO nanoparticles.

Green Synthesis of $CeNiO_3$ Nanocomposite

Cerium nitrate and nickel nitrate solutions, each with the same concentration, were prepared in deionized water and then mixed while stirring. The plant extract was added slowly to the metal salt solution, acting as both a reducing and stabilizing agent. The resulting mixture was stirred at a temperature between 70 and 80 °C until a gel-like precipitate formed. Afterward, the precipitate was separated by centrifugation, washed several times with distilled water and ethanol, and then dried at 80 °C. The dried powder was then calcined at 400–600 °C for 3–4 h to obtain crystalline $CeNiO_3$ nanocomposite. Added the addition of the activated carbon material get final composite product of AC/$CeNiO_3$ nanocomposite.

XRD Analysis

The XRD patterns of the samples that were calcined at 500 °C showed diffraction peaks at 2θ values that matched those of activated carbon was present in the planes of (002) and (111) was respectively. The NiO nanoparticles in the (111), (200), (111), and (220) planes, respectively (JCPDS Card No. 89-5881) [5]. Ce/NiO_3 nanoparticles conform to the planes of (311), (111), (200), and (220), which means that the formation fits well with JCPDS Card No. 43-1002 [6]. The observed observations indicate that the synthesis of NiO, and Ce/NiO_3 nanocomposites initiated at a calcination temperature of around 450 °C. The lack of peaks in other phases shows that the products seen in (Fig.1) are very pure. Using the Debye–Scherrer formula (Equation 1) [7], we calculate the different parameters, such as the size of the crystallite in activated carbon, NiO and Ce/NiO_3 nanocomposite. The findings are shown in Table 1.

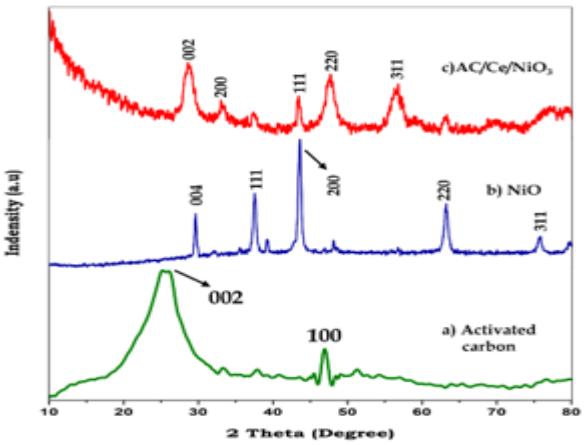

Fig.1 XRD Spectra of (a) Activated carbon, (b) NiO and (c) AC/$CeNiO_3$ nanomaterials

Debye–Scherer's equation

$$\text{Crystalline size (D)} = \frac{0.9\lambda}{\beta \cos\theta} \quad \text{------ (1)}$$

Where λ is the wavelength (λ = 1.5406 Å (Cu Kα), β is the full width half maximum (FWHM) and θ is the diffraction angle.

Table.1. Crystalline size of activated carbon NiO, and Ce/NiO_3 nanocomposite

S.No	Sample	Crystaline Size(nm)
1.	AC	26.5
2.	NiO	32.4
3.	Ce/NiO_3	38.2

Journal of Chemical Health Risks

www.jchr.org

JCHR (2025) 15(6), 3715-3722 | ISSN:2251-6727

FT-IR analysis

The FT-IR technique is a good way to look at the different functional groups in metal oxides, especially those that contain oxygen. Figure 2a shows the FT-IR spectra of activated carbon. They show absorption stretching vibration peaks centered at 467 and 603cm^{-1}, which are thought to be due to Ni-O stretching vibrations. Also, a peak at 1436 cm^{-1} can be due to the stretching of C–O and C=O groups in the metal oxide nanoparticles. The peak at 3549 cm^{-1} also shows the stretching vibrations of H-O-H [8]. The peaks at 467 and 603 cm^{-1} that correspond to the stretching vibrations are due to the stretching mode of the M-O bond (Fig. 2b). The signal at 1631 cm^{-1} also shows that the C–O and C=O groups in the metal oxide nanoparticles are stretching[9]. The peaks at 3562 and 3659 cm^{-1} show how H-O-H stretches. This process stops charge carriers from coming together and causes a synergistic effect that makes the nanocomposite's catalytic activity stronger.

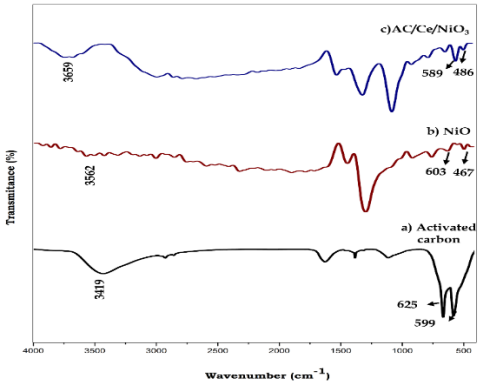

Fig.2 FT-IR spectra of (a) Activated carbon, (b) NiO and (c) AC/CeNiO$_3$ nanomaterials

Morphology analysis

The surface morphology of the produced Activated Carbon, NiO, and CeNiO$_3$ nanocomposite was analyzed using SEM micrographs, depicted in Fig. 3a,3b and 3c, which show the SEM images of activated carbon, NiO and CeNiO$_3$ nanomaterials. The activated carbon nanoparticle exhibited a layer-like structure (Fig. 3a) [10], whereas the NiO nanoparticles had an irregular shape (Fig. 3b) [11]. Ce/NiO$_3$ nanoparticles have an evenly distributed the surface of the activated carbon in many orientations(Fig. 3c).

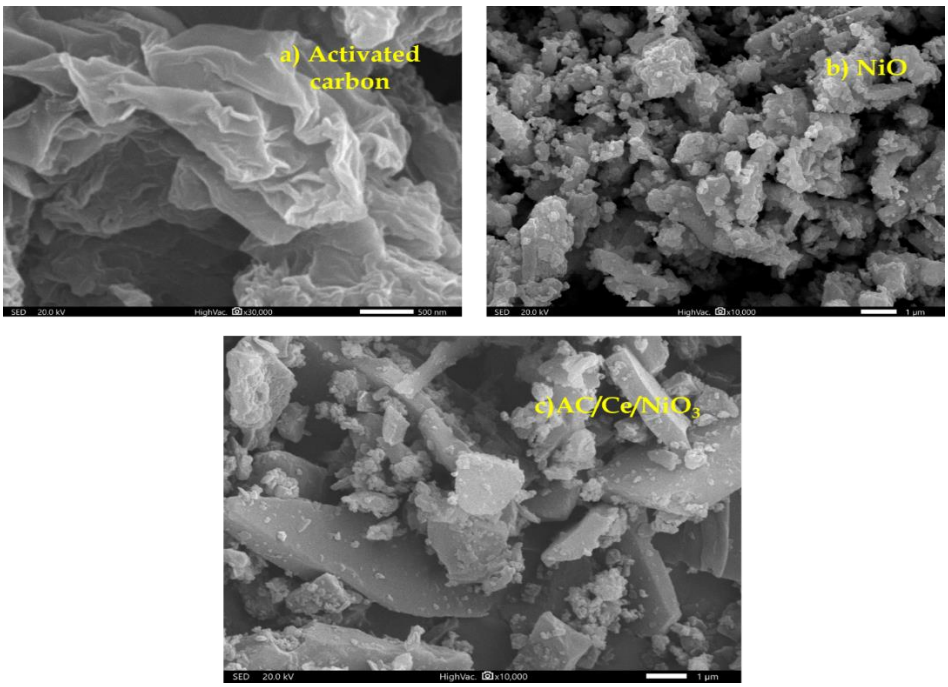

Fig.3 SEM analysis of (a) Activated carbon, (b) NiO and (c) AC/CeNiO$_3$ nanomaterials

Journal of Chemical Health Risks

www.jchr.org

JCHR (2025) 15(6), 3715-3722 | ISSN:2251-6727

Elemental conformation of NiO and AC/Ce/NiO_3 nanocomposite

The elemental composition and purity of the NiO and Ce/NiO_3 nanomaterials that were made were looked at using Energy Dispersive X-ray Spectroscopy (EDS). The EDS spectra show both the presence and amount of the elements in the samples. The EDS spectra of the NiO sample contains unambiguous peaks for nickel (Ni) and oxygen (O)[12]. This means that nickel oxide has formed correctly. The absence of further impurity peaks indicates that the synthesized NiO is quite pure. The atomic and weight percentage numbers show that the ratio of Ni to O is near to stoichiometric. This is another evidence that NiO was manufactured with very little contamination(Fig.4).

The EDS spectra for the Ce/NiO_3 composite reveal unambiguous peaks for oxygen (O), nickel (Ni), and cerium (Ce). The existence of Ce peaks shows that cerium was successfully added to the NiO matrix. The distribution of the components and the fitted ratios we found suggest that Ce and NiO_3 work well together without creating any undesirable secondary phases. There were no more elemental peaks observed, which means that the composite compound is chemically pure[13].

The EDS results reveal that both NiO and Ce/NiO_3 nanomaterials were synthesized correctly, contain the exact quantity of each element, and are pure. This implies they might be utilized for other important things, such photocatalysis, adsorption, and cleaning up the environment.

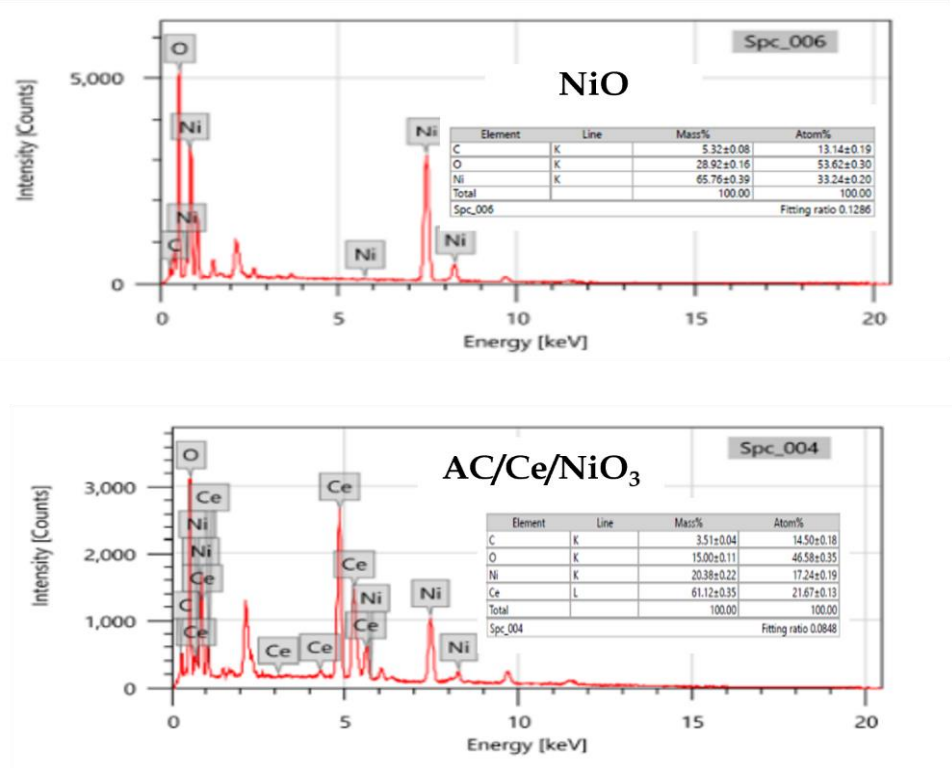

Fig. Elemental conformation of NiO and $CeNiO_3$ nanocomposite

UV - DRS Analysis of NiO and AC/$CeNiO_3$ nanocomposite

Figure 4 presents the UV-diffuse reflectance spectroscopy of NiO and AC/$CeNiO_3$ nanocomposite nanoparticles, demonstrating that pure NiO and AC/$CeNiO_3$ nanoparticles exhibit a pronounced UV absorption edge ranging from 200 to 800 nm. But the UV absorption of the other samples moved to the longer wavelength range. The variations in the absorption edges show that the band structure has changed. The bandgap of the samples is established using the Kubelka-Munk function equation[14].

Journal of Chemical Health Risks
www.jchr.org
JCHR (2025) 15(6), 3715-3722 | ISSN:2251-6727

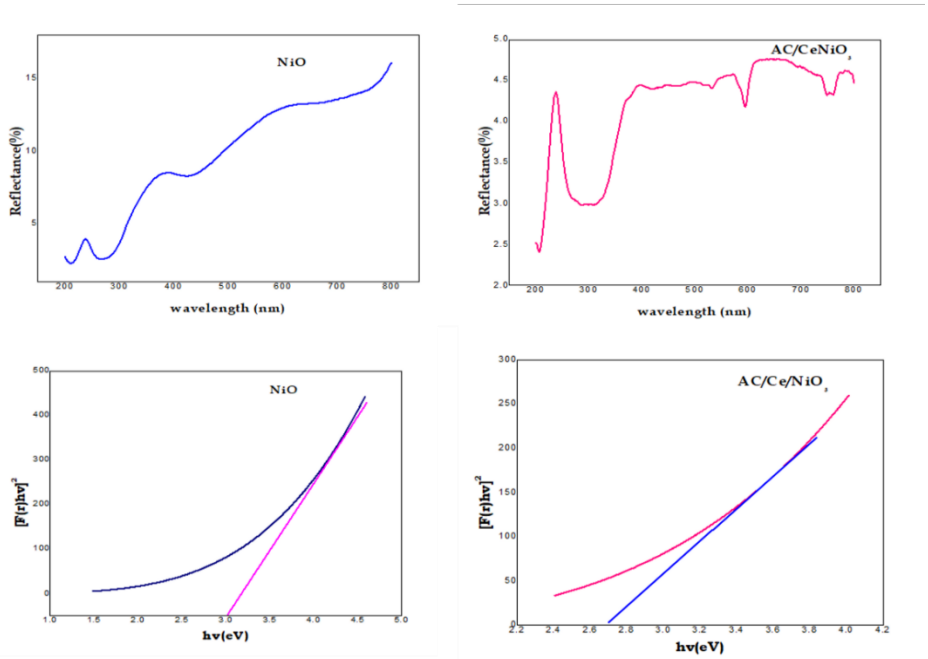

Fig. 4 UV-DRS Image of a)NiO and b) AC/$CeNiO_3$ c) Tauc's plot of NiO and d) Tauc's plot of AC/$CeNiO_3$

$\alpha h\nu = A (h\nu - E_g)n$ ------ (2)

Where α is the absorption coefficient and hν is the energy of the incoming photon. The bandgap energies are calculated from the intersection of the tangents, as shown in Fig. 4. The band gaps of the produced NiO and Ce/NiO_3 nanoparticles were determined to be 3.0 and 2.7 eV, respectively. Oxygen vacancies can cause impurity levels to rise near the valence bond. Ce/NiO_3 has a lower band gap value and is more catalytic than NiO_2 material [15].

Photocatalytic Measurements

The degradation of methylene blue dye solutions as a model organic pollutant under visible light and sunlight was employed to evaluate the photocatalytic activity efficiency of the synthesized NiO and $CeNiO_3$ nanocomposite. It took 60 minutes to break down the dye with sunlight (Fig. 5) [16]. The $CeNiO_3$ nanocomposite developed has showed a faster rate of dye degradation than a pure NiO catalyst. Figure 5a shows that the pure NiO nanoparticle can break down methylene blue with a success rate of 90.0%. The $CeNiO_3$ composite, on the other hand, breaks down 95.0% of methylene blue after 60 minutes of sunshine exposure (Fig. 5a and b) [17].

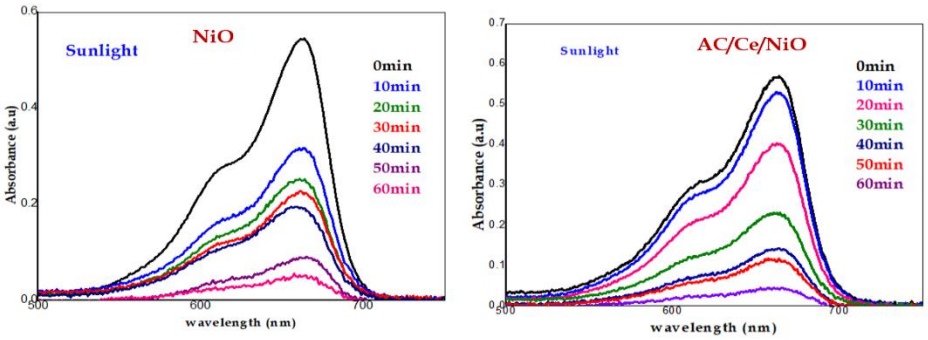

Fig. 5 UV-Vis spectra of a)NiO and b)AC/$CeNiO_3$ under sunlight irradiation.

Journal of Chemical Health Risks

www.jchr.org

JCHR (2025) 15(6), 3715-3722 | ISSN:2251-6727

To see how well the nanoparticles broke down, we utilized 30 mg of the catalyst as a weight percentage. Sunlight exposure was employed to find out how well the elimination worked. Figures 5a and 5b illustrate how well the materials break down when exposed to UV and sunshine. The AC/Ce/NiO_3 material breaks down more quickly than the bare materials (NiO). Every ten minutes, the degradation efficiency was measured, and under solar radiation, the composite AC/Ce/NiO_3 material outperformed NiO nanoparticles[18].

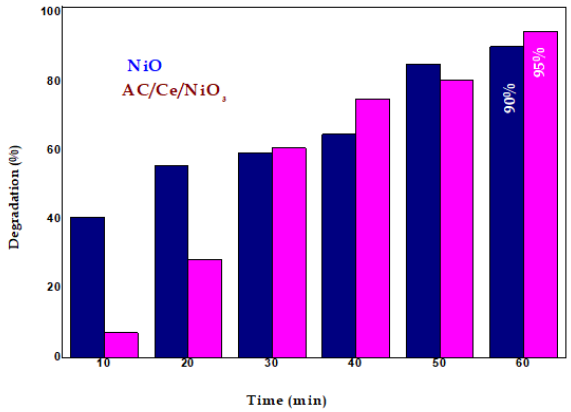

Fig.6 Photocatalytic degradation efficiency of methylene blue dye by using 20mg of catalyst under sunlight irradiation.

Mechanisms of photocatalysis

When NiO and $CeNiO_3$ nanoparticles are exposed to light energy that meets or exceeds their band gap energy, conduction band electrons (e−) and valence band holes (h+) are generated. Creating superoxide radicals speeds up reduction and oxidation reactions, while creating hydroxyl radicals speeds up the oxidation of organic molecules [19]. Figure 6 offers a picture of how the deteriorate ion process works. The notion that heterogeneous photocatalysis initiates the oxidation route of chemical compounds through the generation of hydroxyl radicals. The dye can be changed into the superoxide radical anion O_2.-, or the electrons that are generated by light can join with electron acceptors like O_2.- that are stuck to the surface or dissolved in water[20]. The holes created by the light can oxidize organic molecules by interacting with OH- or H_2O to make .OH radicals. Because it is a strong oxidant, the OH- radical can turn most of the MB into harmless byproducts like CO_2, H_2O, and mineralized product [21].

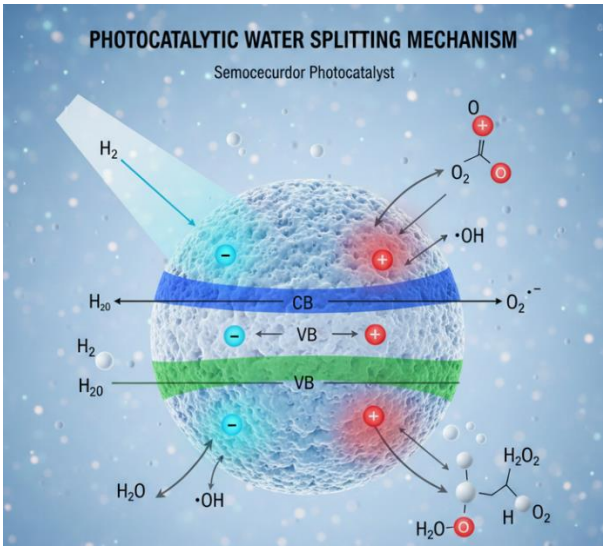

Fig. 7 Mechanisms of photodegradation

Conclusion

A green synthesis approach was used to make activated carbon, NiO, and AC/$CeNiO_3$ nanomaterials. The materials produced activated carbon, NiO, and AC/CeNiO3 nanomaterials after being heated at 500°C for six hours. The crystals had diameters of 26.5, 32.4, and 38.2 nm, respectively. We utilized scanning electron microscopy (SEM) to look at the surface morphology. It showed that NiO and Ce/NiO_3 nanoparticles, which were not structured like anything else, were spread out throughout the surface of the activated carbon, which had a two-dimensional sheet structure. Using the Kubelka-Munk function, we found that the band gap energies for NiO and AC/$CeNiO_3$ were 3.0 eV and 2.7 eV, respectively. We tested the photocatalytic activity of both NiO and AC/$CeNiO_3$ photocatalysts by utilizing sunlight as the light source and methylene blue dye as the target compound. The AC/$CeNiO_3$ nanocomposite degraded faster, reaching 95% degradation, whereas the NiO nanocomposite only reached 90% degradation.

Reference:

1. Nkele, A. C., Alshoaibi, A., Matthew, F. D., Awada, C., Islam, S., & Ezema, F. I. (2025). Synthesis and characterization of sol-gel processed GO/NiO hybrid composites for gas sensing and

photocatalytic applications. *Journal of Sol-Gel Science and Technology*, *114*(3), 874-884.

2. Matthew, D. F., Ahemad, H. I., Aher, Y. B., Sonawane, L. D., More, M. A., Shinde, S. D., ... & Patil, G. E. (2025). Synthesis and characterization of ZnO–NiO binary nanocomposites by hydrothermal technique for gas sensing and photocatalytic applications. *International Journal of Modern Physics B*, *39*(14), 2550109.
3. Puttaraju, T. D., T. L. Soundarya, G. Nagaraju, K. Lingaraju, M. V. Manjula, S. Devaraja, and M. Manjunatha. "Biogenic approach for synthesis of ZnO/NiO nanocomposites as a highly efficient photocatalyst and evaluation of their biological properties." *Brazilian Journal of Chemical Engineering* 42, no. 1 (2025): 95-108.
4. Gnanam, S., Shynu, R. K., Gajendiran, J., Ramya, J. R., Thennarasu, G., Arul, K. T., ... & Kumar, G. R. (2024). Synthesis and characterization of ZnO-NiO nanocomposites for photocatalytic and electrochemical storage applications. *Ionics*, *30*(10), 6653-6665.
5. Yadav, S., Yadav, J., Kumar, M., & Saini, K. (2022). Synthesis and characterization of nickel oxide/cobalt oxide nanocomposite for effective degradation of methylene blue and their comparative electrochemical study as electrode material for supercapacitor application. *International Journal of Hydrogen Energy*, *47*(99), 41684-41697.
6. Anitha, S., Suganya, M., Prabha, D., Srivind, J., Balamurugan, S., & Balu, A. R. (2018). Synthesis and characterization of NiO-CdO composite materials towards photoconductive and antibacterial applications. *Materials Chemistry and Physics*, *211*, 88-96.
7. Kannan, K., Radhika, D., Nesaraj, A. S., Sadasivuni, K. K., & Krishna, L. S. (2020). Facile synthesis of NiO-CYSO nanocomposite for photocatalytic and antibacterial applications. *Inorganic Chemistry Communications*, *122*, 108307.
8. Paul, D., Maiti, S., Sethi, D. P., & Neogi, S. (2021). Bi-functional NiO-ZnO nanocomposite: Synthesis, characterization, antibacterial and photo assisted degradation study. *Advanced Powder Technology*, *32*(1), 131-143.
9. Marand, S. A., Almasi, H., & Marand, N. A. (2021). Chitosan-based nanocomposite films incorporated with NiO nanoparticles: Physicochemical, photocatalytic and antimicrobial properties. *International Journal of Biological Macromolecules*, *190*, 667-678.
10. Saravanakkumar, D., Karthika, R., Ganasaravanan, S., Sivaranjani, S., Pandiarajan, S., Ravikumar, B., & Ayeshamariam, A. (2018). Synthesis of NiO doped ZnO/MWCNT Nanocomposite and its charecterization for photocatalytic & antimicrobial applications. *J. Appl. Phys*, *10*(3), 73-83.
11. Juma, A. O., Arbab, E. A., Muiva, C. M., Lepodise, L. M., & Mola, G. T. (2017). Synthesis and characterization of CuO-NiO-ZnO mixed metal oxide nanocomposite. *Journal of alloys and compounds*, *723*, 866-872.
12. Al-Shawi, S. G., Andreevna Alekhina, N., Aravindhan, S., Thangavelu, L., Elena, A., Viktorovna Kartamysheva, N., & Rafkatovna Zakieva, R. (2021). Synthesis of NiO nanoparticles and sulfur, and nitrogen co doped-graphene quantum dots/nio nanocomposites for antibacterial application. *Journal of Nanostructures*, *11*(1), 181-188.
13. Yasin, A., Hussain, T., Ahmad, R., Shuaib, U., Amjad, M., Ahmad, S., & Imranullah, M. (2023). Photocatalytic and antibacterial potential of chitosan supported nickel oxide/zinc oxide composite synthesized by alcohothermal method. *Water, Air, & Soil Pollution*, *234*(9), 592.
14. Malathi, M., Kaliammal, R., Valarmathi, B., Rajeswari, B., Muthulakshmi, V., Vinoth, K., & Sambasivam, S. (2023). Fenugreek seeds extract mediated nickel oxide nanoparticles and their potential biomedical applications. *Inorganic Chemistry Communications*, *158*, 111699.
15. Lamba, P., Singh, P., Singh, P., Kumar, A., Singh, P., Bharti, ... & Gupta, M. (2021). Bioinspired synthesis of nickel oxide nanoparticles as electrode material for supercapacitor applications. *Ionics*, *27*(12), 5263-5276.
16. Tamesgen, T., Ameya, M. A., Sisay, G., Yuanqi, L., Kai, Z., & Beyene, T. T. (2025). Harnessing the Power of S/N Doped NiO Nanoparticles: Bandgap Tuning for Superior Photocatalytic and Antibacterial Performance.

17. Zarrintaj, P., Khalili, R., Vahabi, H., Saeb, M. R., Ganjali, M. R., & Mozafari, M. (2019). Polyaniline/metal oxides nanocomposites. In *Fundamentals and emerging applications of polyaniline* (pp. 131-141). Elsevier.
18. Long, S., Hui, L., Yanli, D., Dongdong, Z., Feixiong, D., & Weibing, W. (2024). Assessment of antiproliferative activity of green-synthesized nickel oxide nanoparticles against glioblastoma cells using Terminalia chebula. *Green Processing and Synthesis*, *13*(1), 20230112.
19. Lohitha, T., & Albert, H. M. (2025). Biosynthesis, structural, spectroscopic, photoluminescence, and antifungal activity of Ni-doped CeO_2 nanoparticles. *Journal of Fluorescence*, *35*(6), 4183-4196.
20. Muthukumaran, P., Raju, C. V., Sumathi, C., Ravi, G., Solairaj, D., Rameshthangam, P., & Alwarappan, S. (2016). Cerium doped nickel-oxide nanostructures for riboflavin biosensing and antibacterial applications. *New Journal of Chemistry*, *40*(3), 2741-2748.
21. Khyrun, S. F., Christy, A. J., Mayandi, J., & Sagadevan, S. (2023). Photo-triggered antibacterial and catalytic activities of solution combustion synthesized CeO_2/NiO binary nanocomposite. *Inorganic Chemistry Communications*, *153*, 110860.